

# Scalable NAS with Factorizable Architectural Parameters

Lanfei Wang<sup>1\*</sup> Lingxi Xie<sup>2</sup> Tianyi Zhang<sup>3</sup> Jun Guo<sup>1</sup> Qi Tian<sup>2</sup>

<sup>1</sup>Beijing University of Posts and Telecommunications

<sup>2</sup>Huawei Noah's Ark Lab <sup>3</sup>Tsinghua University

wanglanfei@bupt.edu.cn 198808xc@gmail.com tianyi-z16@mails.tsinghua.edu.cn

guojun@bupt.edu.cn tian.qil@huawei.com

## Abstract

Neural architecture search (NAS) is an emerging topic in machine learning and computer vision. The fundamental ideology of NAS is using an automatic mechanism to replace manual designs for exploring powerful network architectures. One of the key factors of NAS is to scale-up the search space, e.g., increasing the number of operators, so that more possibilities are covered, but existing search algorithms often get lost in a large number of operators. This paper presents a scalable NAS algorithm by designing a factorizable set of architectural parameters, so that the size of the search space goes up quadratically while the burden of optimization increases linearly. As a practical example, we add a set of activation functions to the original set containing convolution, pooling and skip-connect, etc. With a marginal increase in search costs and no extra costs in retraining, we are able to find interesting architectures that were not explored before, and achieve state-of-the-art performance in CIFAR10 and ImageNet, two standard image classification benchmarks.

## 1. Introduction

Neural architecture search (NAS) is an important sub-area of automated machine learning (AutoML), which has been attracting increasing attentions in the community of computer vision. It aims to change the conventional, manual way of designing network architectures, and explore the possibility of finding effective architectures automatically in a large search space. Recent years have witnessed a blooming development of NAS, and automatically discovered architectures have surpassed manually designed ones in a wide range of vision tasks, e.g., image classification [57, 29, 46], object detection [13, 12], semantic segmentation [28], etc.

\*This work was done when the first author was an intern at Huawei Noah's Ark Lab.

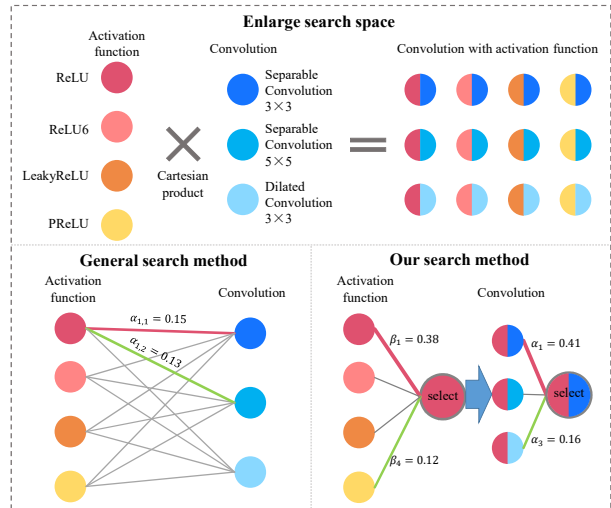


Figure 1. The ideology of this paper is to factorize a large search space (top,  $4 \times 3$  operators) into two (or more) small spaces (bottom, 4 and 3 operators, respectively), so as to avoid the competition between similar operators and ease the search algorithm. In the bottom, red and green segments indicate the best and second-best operators, respectively.

There are two main factors of NAS, namely, architecture sampling and evaluation. The heuristic search approaches, including using reinforcement learning [56, 57, 29] and genetic algorithms [39, 48, 38] for sampling, often required an individual stage for evaluating the sampled architectures, while the so-called one-shot approaches [14, 31, 36] combined two stages into one so that the search process is much faster and thus can be applied to larger search spaces.

This paper continues the efforts in scaling up the search space of NAS. We follow the path of differentiable architecture search, in particular, a recent algorithm named DARTS [31]. By optimizing a super-network efficiently, DARTS has the potential of exploring a large space, but the instability of search, hinders it from being generalized to even more complicated scenarios, e.g., with a larger number of operators. Our observation suggests that one of the

main reason of instability, in a large space, lies in the limited ability of discriminating among an increasing number of operators, since some operators share similar properties and thus forcing them to compete can confuse the search algorithm and lead to sub-optimal results. A toy example is shown in Figure 1.

Motivated by this insight, our idea is straightforward, *i.e.*, designing a **factorizable** set of architectural parameters, so that the operators directly competing with each other are more likely to be distinguishable. In particular, we explore an example that the operator set is the Cartesian product of an **activation operator** group (*e.g.*, ReLU, PReLU, SELU, *etc.*) and a **working operator** group (*e.g.*, sep-conv-3x3, sep-conv-5x5, dil-conv-3x3, *etc.*). In other words, each activation operator can be combined with each working operator, but the weights of all operators are determined separately in the corresponding group. Consequently, the number of possibilities of the ‘final’ operator (a complete activation-working operator) goes up quadratically with the number of trainable architectural parameters increasing linearly. It largely alleviates the burden, as shown in Figure 1, and creates a relatively fair environment for the search process.

We build our experiments on the original DARTS implementation, with the only difference that the search space is defined by a factorizable set of operators, *i.e.*, nine original working operators (including `none`) and nine activation operators (including the originally default ReLU). Consequently, the original DARTS space is enlarged from  $1.1 \times 10^{18}$  to  $9.3 \times 10^{29}$ , enabling us to discover a lot of architectures that have not been studied before. Moreover, since the activation operators are efficient to calculate, the modified framework only needs 20% extra search time on CIFAR10, and no additional costs in both the re-training and inference stages. Experiments are performed on CIFAR10 and ImageNet, two standard image classification benchmarks, on which our approach outperforms the DARTS baseline by a significant margin (a 97.60% accuracy on CIFAR10, and 75.9% top-1 accuracy on ImageNet). Our approach is also friendly to PC-DARTS [52], a recently published variant of DARTS that directly searches on ImageNet, on which we report better performance (76.2% top-1 accuracy) meanwhile preserving the fast search speed.

The remainder of this paper is organized as follows. Section 2 briefly reviews the previous literature, and Section 3 illustrates our approach. Extensive experiments are shown in Section 4 and conclusions drawn in Section 5.

## 2. Related Work

Deep neural networks have been dominating in the field of computer vision. By stacking a large number of convolutional layers and carefully designing training strategies, manually designed networks [26, 16, 20, 51] achieved great

successes in a wide range of applications. However, the number of artificial architectures is still small, and it is widely believed that these architectures are prone to be sub-optimal. Recently, neural architecture search (NAS) has attracted increasing attentions from both academia and industry [41, 17]. As an emerging topic of AutoML, NAS originates from the motivation that powerful architectures can be found by automatic algorithms, provided that the search space is large enough [56]. Besides neural architectures, researchers also designed effective algorithms to search for other parameters, such as activation functions [37] and data augmentation policies [7].

There are typically two pipelines of NAS, which differ from each other in how the search module (sampling architectures from the search space) interacts with the optimization module (evaluating the sampled architectures). The first pipeline isolated search from optimization, with the search module learning a parameterized policy of sampling architectures, and the optimization module providing rewards by training the sampled architecture from scratch. The search policy can be formulated with either reinforcement learning [56, 57, 36, 3] or evolutionary algorithms [39, 48, 38]. Towards a higher search efficiency, researchers proposed to construct a super-network [57, 45, 47, 41, 42] to reduce the search space, or approximated the search space with modified strategies [17, 29, 11, 12].

However, the above pipeline suffers the difficulty of being computationally expensive, *e.g.*, requiring hundreds or even thousands of GPU-days. To accelerate, researchers moved towards jointly optimizing the search and optimization modules. After research efforts in sharing computation among individual optimization [3, 36], the second pipeline, known as the one-shot method, was proposed. A representative work is DARTS [31] which formulated architecture search in a differentiable manner so that end-to-end optimization was made possible. Despite efficiency, DARTS suffers the issue of instability, which was somewhat alleviated by follow-up variants [10, 5, 42, 47] which mostly worked in the original DARTS search space which is of a limited scale. Back to the ideology of NAS, expanding the search space is always a pursuit, yet researchers worried that current differentiable search algorithms will get lost in a large space [2, 53]. In this paper, we focus on investigating a relatively safe manner to enlarge the search space for the neural architecture search.

## 3. Our Approach

### 3.1. Preliminaries: The DARTS Algorithm

The fundamental idea of DARTS is to formulate NAS into a process of super-network optimization, in which the super-network is a mathematical function  $f(\mathbf{x}; \omega, \alpha)$ , in which  $\mathbf{x}$  denotes the input,  $\omega$  indicates the network param-

ters (e.g., convolutional weights) and  $\alpha$  indicates the architectural parameters (i.e., the weights of different operators). The goal is to find the optimal  $\alpha$  which determines the preserved sub-network (the final architecture), and  $\omega$  is jointly trained to assist the optimization of  $\alpha$ .

The basic network of DARTS is stacked by a number of **cells**, each of which has a few nodes (indicating network layers with trainable operators) connected by the edges between them (indicating whether the output of one node is used as the input of another). In particular, let there be  $N$  nodes, and the default topology determines that node  $i$  can send information to node  $j$  if and only if  $i < j$ . Each node collects input data from the nodes with lower indices, and perform a mixed operation

$$f_{i,j}(\mathbf{x}_i) = \sum_{o \in \mathcal{O}} \frac{\exp\{\alpha_{i,j}^o\}}{\sum_{o' \in \mathcal{O}} \exp\{\alpha_{i,j}^{o'}\}} \cdot o(\sigma(\mathbf{x}_i)), \quad (1)$$

where  $\mathcal{O}$  is the set of selectable operators and  $o$  is an element in it. On each edge  $(i, j)$ ,  $\alpha_{i,j}^o$  is the weight of the operation  $o(\sigma(\mathbf{x}_i))$ , and  $\sigma(\cdot)$  denotes the default activation function, i.e., ReLU [35] ( $\sigma(\mathbf{x}) = \max\{\mathbf{x}, \mathbf{0}\}$ , where  $\max$  performs an element-wise operation). The output of a node is the sum of all input flows, i.e.,  $\mathbf{x}_j = \sum_{i < j} f_{i,j}(\mathbf{x}_i)$ , and the output of the entire cell is the concatenation of the outputs of all nodes  $\{\mathbf{x}_2, \dots, \mathbf{x}_{N-1}\}$ . Following the convention of DARTS, the first two nodes,  $\mathbf{x}_0$  and  $\mathbf{x}_1$ , are input nodes to a cell and do not appear in the output.

To train the super-network  $f(\mathbf{x}; \omega, \alpha)$ , with respect to both  $\omega$  and  $\alpha$ , a bi-level optimization algorithm is adopted. In each training epoch, the first part optimizes  $\omega$  with the current  $\alpha$  fixed, and the second part updates  $\alpha$  with the new  $\omega$ . This process repeats iteratively until convergence or a pre-defined training rounds have been performed.

### 3.2. Enlarging the Search Space with a Factorizable Set of Operators

Our goal is to enlarge the space so that the search algorithm can explore more possibilities. A straightforward idea is to introduce new operators to space, i.e., using a larger set of  $\mathcal{O}$ . However, as more operators are added, there may exist similar operators, yet expected to compete with each other. In this situation, the scores assigned to these operators can be quite close, and so small noise in optimization can alter the final choice among them. As a result, the stability of the search algorithm is reduced.

Our solution is intuitive, which represents each operator in the large set,  $\mathcal{O}$ , into a combination of two operators in the smaller sets,  $\mathcal{O}_1$  and  $\mathcal{O}_2$ , respectively<sup>1</sup>. In other words,  $\mathcal{O} \subseteq \mathcal{O}_1 \times \mathcal{O}_2$ , where  $\times$  denotes the Cartesian product. In

<sup>1</sup>This framework is easily generalized to the scenario that  $\mathcal{O}$  is factorized into multiple sets, but throughout this paper, two sets are used.

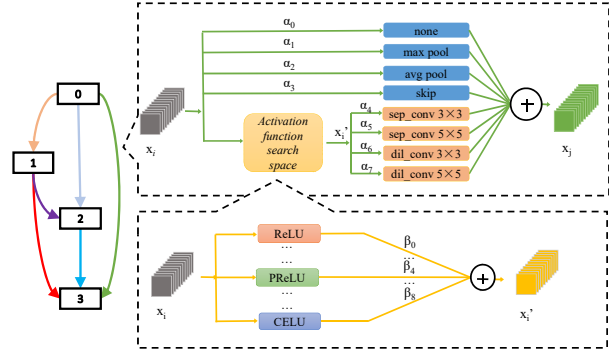


Figure 2. The modified cell structure. On each edge of the cell, the candidate normal operators are partitioned into two groups, i.e., parameterized and non-parameterized. The former is equipped with a set of candidate activation functions while the latter is not. The mixed-activation operator provides the input of the first group.

this way, we expect the factorized operators in  $\mathcal{O}_1$  and  $\mathcal{O}_2$  to be easier discriminated than those in  $\mathcal{O}$ .

The benefit of factorization can be also understood from a reduced number of architectural parameters. Since these parameters are typically more difficult to optimize compared to the weight parameters (e.g., convolutional weights), reducing the amount of them improves the stability of the search process.

### 3.3. Activation Function Search: An Example

As a practical example, we assume  $\mathcal{O}_1$  to be the operator set used in the original DARTS algorithm, and  $\mathcal{O}_2$  to be a set of **activation functions**. Note that in the original DARTS algorithm, ReLU [35] was used as the default activation function, added before each convolutional operation (i.e., sep-conv-3x3, sep-conv-5x5, dil-conv-3x3, and sep-conv-5x5). We note that researchers proposed other solutions (e.g., the searched activation function, Swish [37]), most of which were verified stronger than ReLU. Therefore, we are interested in (i) whether these functions can be integrated into a differentiable NAS framework like DARTS, and (ii) whether applying a mixture of activation functions is better than using a fixed one.

To explore these possibilities, we choose nine popular activation functions from the previous literature, namely, four variants of ReLU (i.e., ReLU6 [24], LeakyReLU [34], PReLU [15] and RReLU [50], differing from the original version in the strategy of dealing with negative and saturating-positive responses) and three variants of ELU (i.e., ELU [6], CELU [1] and SELU [23], also with subtle differences from each other). The last one is Swish [37], which is in the form of  $x \times \sigma(b \cdot x)$  where  $\sigma(\cdot)$  is the sigmoid function and  $b$  is the learned coefficient. Of course, it is possible to introduce other options such as the vanilla sigmoid, but we ignore them because they are often less effective in deep neural networks. A cell structure in the

modified super-network is shown in Figure 2. Since each pair of activation function and convolutional operation can cooperate, there are a total of  $9 \times 4 + 4 = 40$  operators in  $\mathcal{O}$ , including the dull operator `none` (*a.k.a.*, `zero`). Our formulation provides an opportunity to explore a large space without forcing them to compete in one stage.

One may worry that the activation functions may have similar behaviors (*e.g.*, the difference among the five ReLU-based functions is much smaller than that among the four convolution-based operations), so that the difficulty of discriminating them in the search process is large. We make two comments here. On the one hand, in experiments, we find that the weights on these functions are even easier to converge and the advantage of the ‘maximal’ function is often large. On the other hand, if two or more similar activation functions are difficult to discriminate, we believe that their properties are indeed very similar, so the performance of the searched architecture will be good with either of them preserved.

### 3.4. Tri-Level Optimization

With two sets,  $\mathcal{O}_1$  and  $\mathcal{O}_2$ , being used in the formulation, the super-network is written as  $f(\mathbf{x}; \boldsymbol{\omega}, \boldsymbol{\alpha}, \boldsymbol{\beta})$ , in which  $\boldsymbol{\beta}$  denotes the weights of the newly-added set of architectural parameters. Hence, Eqn (1) becomes:

$$f_{i,j}(\mathbf{x}_i) = \sum_{o_1 \in \mathcal{O}_1} \frac{\exp\{\alpha_{i,j}^{o_1}\}}{\sum_{o'_1 \in \mathcal{O}_1} \exp\{\alpha_{i,j}^{o'_1}\}} \cdot o_1(\sigma_{i,j}^{o_1}(\mathbf{x}_i)). \quad (2)$$

Note that the activation function has been replaced by  $\sigma_{i,j}^{o_1}(\mathbf{x}_i)$ , which is determined by both  $o_1$  and  $\boldsymbol{\beta}$ . If  $o_1$  falls within the non-parameterized subset of  $\mathcal{O}_1$ , *i.e.*, no activation function is performed before  $o_1(\cdot)$ , we have  $\sigma_{i,j}^{o_1}(\mathbf{x}_i) \equiv \mathbf{x}_i$ , otherwise the output of activation follows a mixture formulation similar to that of normal operations, *i.e.*,

$$\sigma_{i,j}^{o_1}(\mathbf{x}_i) = \sum_{o_2 \in \mathcal{O}_2} \frac{\exp\{\beta_{i,j}^{o_2}\}}{\sum_{o'_2 \in \mathcal{O}_2} \exp\{\beta_{i,j}^{o'_2}\}} \cdot o_2(\mathbf{x}_i). \quad (3)$$

On each edge  $(i, j)$ , the input feature,  $\mathbf{x}_i$ , gets through the parameters of  $\boldsymbol{\beta}$ ,  $\boldsymbol{\omega}$ , and  $\boldsymbol{\alpha}$  orderly and arrives at the output,  $\mathbf{x}_j$ . The overall loss function that minimizes the recognition error,  $\mathbb{E}\left[\|f(\mathbf{x}; \boldsymbol{\omega}, \boldsymbol{\alpha}, \boldsymbol{\beta}) - \mathbf{y}\|^2\right]$  ( $\mathbb{E}[\cdot]$  denotes the expectation). Hence, optimizing the super-network with respect to  $\boldsymbol{\omega}$ ,  $\boldsymbol{\alpha}$  and  $\boldsymbol{\beta}$  involves a tri-level optimization process, which we illustrate in Algorithm 1.

### 3.5. Discussion and Relationship to Previous Work

The main contribution of our work is to provide an efficient way to expand the search space. Technically, the key is to avoid introducing a large number of architectural parameters. But, essentially, the idea is to assume the distribution of the hyper-parameters to be factorizable, so that

---

#### Algorithm 1: Tri-Level Optimization for DARTS Equipped with Activation Functions

---

**Input** : a training set  $\mathcal{T}$ , a validation set  $\mathcal{V}$ , super-network  $f(\cdot; \boldsymbol{\omega}, \boldsymbol{\alpha}, \boldsymbol{\beta})$ , loss functions  $\mathcal{L}_{\text{train}}(\cdot)$  and  $\mathcal{L}_{\text{val}}(\cdot)$ , learning rates  $\eta_\alpha, \eta_\beta$  and  $\eta_\omega$ , number of search epochs  $T$ ;

**Output**: parameters  $\boldsymbol{\alpha}$  and  $\boldsymbol{\beta}$ ;

- 1 Initialize  $\boldsymbol{\alpha}_0, \boldsymbol{\beta}_0$  and  $\boldsymbol{\omega}_0, t \leftarrow 0$ ;
- 2 **while**  $t < T$  **do**
- 3      $\boldsymbol{\omega}_{t+1} \leftarrow \boldsymbol{\omega}_t - \eta_\omega \cdot \nabla_{\boldsymbol{\omega}_t} \mathcal{L}_{\text{train}}(\boldsymbol{\omega}_t, \boldsymbol{\alpha}_t, \boldsymbol{\beta}_t)$ ;
- 4      $\boldsymbol{\alpha}_{t+1} \leftarrow \boldsymbol{\alpha}_t - \eta_\alpha \cdot \nabla_{\boldsymbol{\alpha}_t} \mathcal{L}_{\text{val}}(\boldsymbol{\omega}_{t+1}, \boldsymbol{\alpha}_t, \boldsymbol{\beta}_t)$ ;
- 5      $\boldsymbol{\beta}_{t+1} \leftarrow \boldsymbol{\beta}_t - \eta_\beta \cdot \nabla_{\boldsymbol{\beta}_t} \mathcal{L}_{\text{val}}(\boldsymbol{\omega}_{t+1}, \boldsymbol{\alpha}_{t+1}, \boldsymbol{\beta}_t)$ ;
- 6      $t \leftarrow t + 1$ ;
- 7 **end**

**Return**:  $\boldsymbol{\alpha} \leftarrow \boldsymbol{\alpha}_T, \boldsymbol{\beta} \leftarrow \boldsymbol{\beta}_T$ .

---

we can use greedy search to optimize them individually, or iteratively. From this perspective, this idea is related to PNAS [29], a NAS approach with reinforcement learning as the optimizer.

Throughout this work, we assume that  $\mathcal{O}$  is factorized into two sets, yet this is not a hard limitation of our approach. With more options added to search (*e.g.*, the type of batch normalization, which is appended after each normal operator), complicated factorization is required and there will be the need for increasing the number of levels in optimization. Although this can bring in difficulties in either convergence or stability [2, 53], it provides a chance of enlarging the search space at relatively low risk.

Searching for activation functions enjoys a natural benefit in the efficiency of the searched architectures. That being said, the time and memory costs do not change in the re-training stage (and also, the inference time). Yet, as we shall see later, the accuracy is significantly boosted. Previous work also explored this possibility and discovered `Swish` [37], but it was constrained that all activation functions are the same, whereas our work can assign different activation functions to different positions of the cell. In addition, as we shall see in experiments, `Swish` is not the most effective activation function on DARTS, even under the assumption of all functions being the same.

## 4. Experiments

### 4.1. Basic Setting

The basic setting follows DARTS [31], except for a new set of architectural parameters that have been added. The super-network has 8 stacked cells, 6 of them are normal cells and the remaining 2 are reduction cells, placed after the 2nd and 4th normal cells, respectively. Cells of the same type share the same set of architectural parameters. A normal cell does not change the spatial resolution of the input,

Architecture	Test Error (%)	Params (M)	Search Cost (GPU-days)	Search Method
DenseNet-BC [20]	3.46	25.6	-	manual
NASNet-A [57] + cutout	2.65	3.3	1800	RL
AmoebaNet-A [38] + cutout	3.34±0.06	3.2	3150	evolution
AmoebaNet-B [38] + cutout	2.55±0.05	2.8	3150	evolution
Hierarchical Evolution [30]	3.75±0.12	15.7	300	evolution
PNAS [29]	3.41±0.09	3.2	225	SMBO
ENAS [36] + cutout	2.89	4.6	0.5	RL
NAONet-WS [32]	3.53	3.1	0.4	NAO
DARTS (1st order) [31] + cutout	3.00±0.14	3.3	0.4	gradient-based
DARTS (2nd order) [31] + cutout	2.76±0.09	3.3	1	gradient-based
SNAS (mild) [49] + cutout	2.98	2.9	1.5	gradient-based
SNAS (moderate) [49] + cutout	2.85±0.02	2.8	1.5	gradient-based
SNAS (aggressive) [49] + cutout	3.10±0.04	2.3	1.5	gradient-based
ProxylessNAS [4] + cutout	2.08	-	4.0	gradient-based
P-DARTS [5] + cutout	2.50	3.4	0.3	gradient-based
BayesNAS [54] + cutout	2.81±0.04	3.4	0.2	gradient-based
PC-DARTS [52] + cutout	2.57±0.07	3.6	0.1	gradient-based
A-DARTS (ours) + cutout	2.40±0.08	3.7	0.3	gradient-based

Table 1. Comparison with state-of-the-art architectures on CIFAR10. The accuracy of our approach is reported by averaging 3 individual runs of architecture search. The search cost is reported with a single NVIDIA Tesla-V100 GPU.

and a reduction cell shrinks both the height and width of the input by half. Each cell has 2 input nodes, 4 intermediate nodes and an output node.

We evaluate our approach on two standard image classification benchmarks, namely, the CIFAR10 [25] and ImageNet [8] datasets. Following the convention of DARTS-based approaches [31, 5, 52], we optimize the super-network on the CIFAR10 dataset and, after the sub-network is determined, re-train it on either CIFAR10 or ImageNet datasets. Besides, our approach can be combined with PC-DARTS [52] to search directly on the Imagenet dataset. Detailed configurations are elaborated in the following parts.

## 4.2. Results on CIFAR10

The CIFAR10 [25] dataset contains 60,000 tiny ( $32 \times 32$ ) RGB images, 50,000 for training and 10,000 for testing, both of which are evenly distributed over 10 classes. It is one of the most popular proxy datasets, on which the network architecture is searched and applied elsewhere.

We set the number of search epochs to be 25 as the convergence of our approach, after the activation functions being added, is significantly faster. The training set is partitioned into two equal folds and used in the training and validation stages, respectively. After the search process, we check if there is at least one skip-connect operator in the normal cell, if not, it is discarded. Empirically, an architecture without skip-connect in the normal cell often accumu-

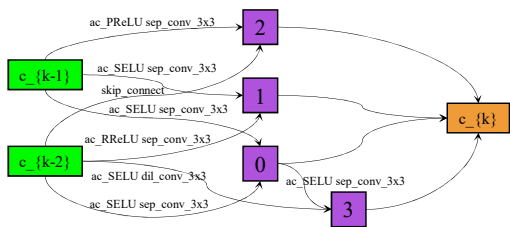
lates accuracy slowly in the re-training stage.

Following the first-order setting of DARTS, we set the basic channel number to be 16, and use a batch size of 64 during the search process. An SGD optimizer is used to optimize the weight parameters ( $\omega$ ), with an initial learning rate of 0.05 and cosine annealed to a minimal value of 0.001. The architectural parameters ( $\alpha$  and  $\beta$ ) are optimized using two Adam optimizers [22] with the same configurations, *i.e.*, a fixed learning rate of  $6 \times 10^{-4}$ , a momentum of (0.5, 0.999) and a weight decay of  $10^{-3}$ . 0.3 GPU-days are required for the entire search process. Regarding other details, please refer to the original paper [31].

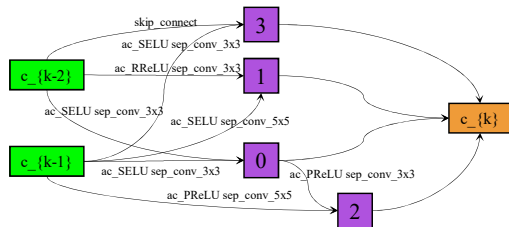
After the search process, the final architecture is re-trained from scratch. We follow the convention to use 18 normal cells and 2 reduction cells, which appear after the 6th and 12th normal cells, respectively. The number of epochs is 600, and the initial channel number is 36. We set the batch size to be 128, and use an SGD optimizer with an initial learning rate of 0.03 (cosine annealed to 0), a momentum of 0.9, a weight decay of  $3 \times 10^{-4}$  and a norm gradient client at 5. DropPath [21, 27] and cutout [9] are also used for re-training, with a dropout rate of 0.4 and an auxiliary weight of 0.4.

- **Comparison to the State-of-the-Arts**

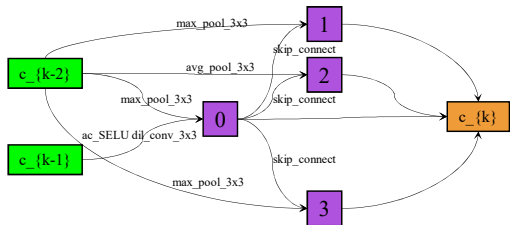
The comparison between our classification accuracy on CIFAR10 and previous work is shown in Table 1. With



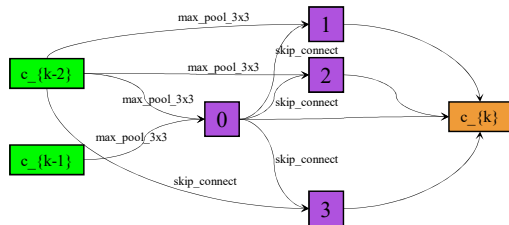
(a) Normal cell: searched on the *free* configuration.



(b) Normal cell: searched on *Config-A*.



(c) Reduction cell: searched on the *free* configuration.



(d) Reduction cell: searched on *Config-A*.

Figure 3. The normal cells and reduction cells found on the CIFAR10 dataset under different settings, namely, the free-search setting (left, using our algorithm to find the optimal  $\alpha$  and  $\beta$  jointly, a test error of 2.40%), and the fixed-search setting (right, fixing the optimal  $\beta$  obtained from the previous search and only optimizing  $\alpha$ , a test error of 2.50%). That being said, these two architectures share the same  $\beta$ , but the preserved edges (determined by  $\alpha$ ) can be different. *Please note the different orders of nodes for the two normal cells.*

only a search cost of 0.3 GPU-days, our approach dubbed A-DARTS achieves an error rate of 2.40%, which ranks among the top of existing DARTS-based approaches. With factorization, our approach produces stable results on the enlarged space: in three individual search processes, the found architectures report 2.40% (as shown in the table), 2.34% and 2.48% average error rates, all of which are competitive. In addition, the searched architecture does not require longer time or larger memory in both re-training and testing stages, *i.e.*, from the perspective of real-world applications, the improvement of accuracy comes for free.

The architecture corresponding to the error rate of 2.40% is shown in the first row of Figure 3(a) and Figure 3(c). The searched normal cell is somewhat similar to that found in PC-DARTS [52] (the max number of cascaded convolutions is 2), unlike that found in P-DARTS [5] which has deeper connections. Also, SELU appears in 5 out of 7 edges (one edge is occupied by skip-connect and thus does not need activation), claiming its dominance over other activation functions. In contrary, Swish [37], the searched activation function, does not appear in any edge, implying that Swish may not be the optimal choice in a generalized setting (in particular, DARTS). As we shall see in the next part, even in the search using a fixed activation function, Swish does not show an advantage over other competitors.

• **Search with Fixed Activation Functions**

Method		Test Error	Params
search with	retrain with	(%)	(M)
ReLU	ReLU	2.67±0.09	3.3
ReLU6	ReLU6	2.65±0.08	3.8
LeakyReLU	LeakyReLU	2.66±0.10	3.9
PReLU	PReLU	2.62±0.10	3.6
RReLU	RReLU	2.59±0.04	3.9
ELU	ELU	2.62±0.08	3.6
SELU	SELU	2.58±0.05	3.8
CELU	CELU	2.62±0.05	4.0
Swish	Swish	2.61±0.20	3.6
<i>Config-A</i>	<i>Config-A</i>	2.50±0.14	4.0
<i>free</i>	ReLU	2.50±0.05	3.7
<i>free</i>	SELU	2.42±0.06	3.7
<i>free</i>	<i>free</i>	2.40±0.08	3.7

Table 2. Comparison of search performance on CIFAR10, between our approach and those with different options fixed, *e.g.*, in the 2nd and 3rd lines from the bottom, we retrain the model by replacing the searched activation functions with the fixed ones.

In this part, we perform diagnostic studies to verify the effectiveness of searching in the enlarged space. **First**, we enumerate all 9 elements in the activation function set and re-run the search process with each of them fixed to be the

Architecture	Test Err.(%)		Params (M)	FLOPS (M)	Search Cost (GPU-days)	Search Method
	top-1	top-5				
Inception-v1 [43]	30.2	10.1	6.6	1448	-	manual
MobileNet [18]	29.4	10.5	4.2	569	-	manual
ShuffleNet 2 × (v1) [33]	26.4	10.2	~5	524	-	manual
ShuffleNet 2 × (v2) [33]	25.1	-	~5	591	-	manual
NASNet-A [57]	26.0	8.4	5.3	564	1800	RL
NASNet-B [57]	27.2	8.7	5.3	488	1800	RL
NASNet-C [57]	27.5	9.0	4.9	558	1800	RL
AmoebaNet-A [38]	25.5	8.0	5.1	555	3150	evolution
AmoebaNet-B [38]	26.0	8.5	5.3	555	3150	evolution
AmoebaNet-C [38]	24.3	7.6	6.4	570	3150	evolution
PNAS [29]	25.8	8.1	5.1	588	225	SMBO
MnasNet-92 [45]	25.2	8.0	4.4	388	-	RL
DARTS (2nd order) [31]	26.7	8.7	4.7	574	4.0	gradient-based
SNAS (mild) [49]	27.3	9.2	4.3	522	1.5	gradient-based
ProxylessNAS <sup>‡</sup> [4]	24.9	7.5	7.1	465	8.3	gradient-based
P-DARTS (CIFAR10) [5]	24.4	7.4	4.9	557	0.3	gradient-based
P-DARTS (CIFAR100) [5]	24.7	7.5	5.1	577	0.3	gradient-based
BayesNAS [54]	26.5	8.9	3.9	-	0.2	gradient-based
PC-DARTS [52]	25.1	7.8	5.3	586	0.1	gradient-based
PC-DARTS <sup>‡</sup> [52]	24.2	7.3	5.3	597	3.8	gradient-based
A-DARTS (ours)	24.1	7.3	5.2	587	0.3	gradient-based
A-PC-DARTS <sup>‡</sup> (ours)	23.8	7.0	5.3	598	6.3	gradient-based

Table 3. Comparison with state-of-the-art network architectures on ImageNet (mobile setting). The symbol of <sup>‡</sup> indicates the corresponding architecture is searched on ImageNet directly, otherwise it is transferred from CIFAR10.

default activation. As shown in Table 2, all these activation functions produce statistically comparable results, with the worst being ReLU<sup>2</sup>, and the best being SELU, *i.e.*, the dominant option in the searched architecture. However, even with SELU fixed, the performance is significantly worse than the searched one. **Second** and oppositely, we leverage the configuration of activation functions from the 2.40%-error architecture (which we call *Config-A*), fix the architectural parameters of activation functions (the  $\beta$  at the end of the previous search) and redo the search (only  $\alpha$  and  $\omega$  are learnable). The accuracy, 2.50%, is still significantly lower than that of free search (2.40%). On the other hand, if we directly use *Config-A* but simply replace the activation functions in the re-training stage (from the searched configuration to fixed options, including ReLU and SELU), the accuracy does not drop much.

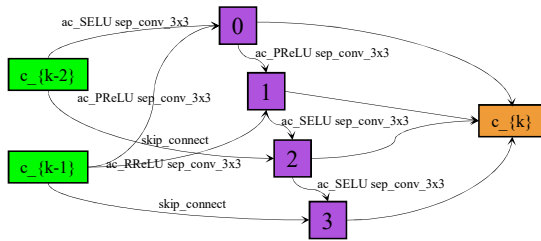
The above results draw an interesting hypothesis that during the search process, the two sets of architectural parameters are prone to impact each other, and the final (op-

timal) architecture is not likely to be found if we fix either part and search only on the reduced space. That being said, being able to explore in a large space is more important than the results obtained from the large space. We acquire this ability by factorizing architectural parameters, which is currently a powerful yet safe solution.

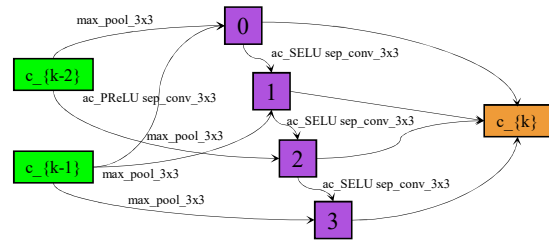
### 4.3. Results on ImageNet

ImageNet [8] is one of the most popular datasets for large-scale image classification. We follow the convention to use a subset of it, usually referred to as ILSVRC2012 [40] for experiments. ILSVRC2012 contains 1,000 object classes and around 1.3M training images. All the images are of a high-resolution, crawled from the Internet, and labeled in a crowd-sourcing manner. The test set (the original validation set released by the authors) contains 50 images for each class or 50K images in total. There are typically two ways to obtain the architecture for ImageNet. One is to search the architecture on a *proxy* dataset then transfer it to ImageNet, and the other is to directly search the architecture on ImageNet, known as the *proxyless* setting [4, 52]. Here, we investigate both options. For the former setting, we use CIFAR10 as the proxy dataset, which produces an architec-

<sup>2</sup>Note that when we choose ReLU, the search degenerates to the original DARTS approach. However, our accuracy (2.67%) is higher than that (3.00%) of DARTS, mainly due to the improved search configuration, which we borrowed from previous work [5, 52].



(a) Normal cell: searched using PC-DARTS.



(b) Reduction cell: searched using PC-DARTS.

Figure 4. The normal cell (left) and reduction cell (right) of the architecture found on ImageNet.

ture with a 2.40% testing error, as shown in Figure 3.

Regarding the proxyless setting (*i.e.*, search on ImageNet directly), we follow PC-DARTS [52] to sample a subset from the original training set, with the training and validation set containing 10% and 2.5% images, respectively, and all classes preserved. A total of 50 epochs are used for architecture search, and the first 15 epochs are used for warm-up. To train the network weights,  $\omega$ , a momentum SGD is used, with the learning rate starting from 0.5 and gradually annealed down to 0 in a cosine schedule (without restart). The momentum is 0.9, the weight decay is  $3 \times 10^{-5}$ . To train the architectural weights,  $\alpha$  and  $\beta$ , we use two Adam optimizers [22] with a fixed learning rate of  $6 \times 10^{-3}$ , a momentum (0.5, 0.999) and a weight decay of  $10^{-3}$ . We run the program on 8 NVIDIA Tesla-V100 GPUs. Following PC-DARTS to sub-sample 1/2 channels at each time, the batch size can be as large as 1,024. The entire search process takes around 19 hours, slightly longer than PC-DARTS.

For both proxy and proxyless settings, the searched architectures have 8 cells, 6 normal cells and 2 reduction cells, and we deepen the network by doubling the number of normal cells at each stage, resulting in a 14-cell network. The number of initial channels is computed so that the total FLOPs does not exceed 600M.

We also use 8 NVIDIA Tesla-V100 GPUs to re-train the transferred architectures for 250 epochs from scratch, with the batch size of 512. The network parameters are optimized by a SGD optimizer with an initial learning rate of 0.25 (gradually annealed to close to 0 following the cosine setting), a momentum of 0.9 and a weight decay of  $3 \times 10^{-5}$ . Default enhancements are also used, including label smoothing [44] and an auxiliary loss tower, and the auxiliary weight is 0.2. As the batch size is large, the learning rate rises linearly to 0.5 in the first 5 epochs, which is known as a warm-up stage.

### • Comparison to the State-of-the-Arts

Results are summarized in Table 3. In both the proxy and proxyless settings, our approach demonstrates state-of-

Method		Test Error.(%)		Params
search with	retrain with	top-1	top-5	(M)
ReLU	ReLU	24.9	7.4	5.2
SELU	SELU	24.6	7.3	5.1
<i>free</i>	ReLU	24.5	7.4	5.2
<i>free</i>	SELU	24.3	7.3	5.2
<i>free</i>	<i>free</i>	24.1	7.3	5.2

Table 4. Comparison of search performance, on ImageNet, between our approach and those with different options fixed, *e.g.*, in the 2nd and 3rd lines from the bottom, we retrain the model by replacing the searched activation functions with the fixed ones. Please refer to Table 2 for the corresponding results on CIFAR10.

the-art performance. In particular, in the proxy setting, the top-1 error rate of 24.1% surpasses all published DARTS-based results. Note that our approach was built on the original DARTS algorithm, which has a relatively weak ability. When we combine our approach with PC-DARTS, a strong baseline which was published recently, the classification error continues to drop. Without bells and whistles (*e.g.*, the squeeze-and-excitation [19] module and AutoAugment [7] which were verified effective), we arrive at a top-1 error of 23.8%, which surpasses PC-DARTS by a margin of 0.4%. This verifies that the idea of factorizing the search space is generalized to other search algorithms.

The searched architectures, using PC-DARTS, are visualized in Figure 4. Unlike those found on CIFAR10, this architecture has much deeper connections, *i.e.*, 4 cascaded convolutional layers exist in both normal cell and reduction cell. Still, SELU was chosen most, and both PReLU and RReLU contributed to the improvement.

### • Search with Fixed Activation Functions

As in CIFAR10, we perform experiments to search with fixed activation functions. Results are shown in Table 4. Again, our approach outperforms other options with fixed activation functions in either the re-training stage or both



the search and re-training stages, which supports our discussions and hypothesis made in the CIFAR10 experiments.

## 5. Conclusions

In this paper, we present an efficient yet effective approach to enlarge the search space, so that the NAS algorithms have the potential of improvement by exploring a larger number of possibilities. The idea is to factorize a search space into two (or even more) sets of architectural parameters, so that the number of combinations increases super-linearly with the learnable architectural parameters increasing linearly, which reduces both computational overhead and optimization difficulty. Experiments on CIFAR10 and ImageNet demonstrate superior performance beyond the state-of-the-art of DARTS-based methods, and diagnostic experiments verify the benefits of using a large search space.

This research puts forward a new path that helps to augment the search space which, in the current era, may incur instability due to the inaccuracy in optimization [2, 53]. Our work leaves a lot of issues to be solved. For example, it remains unclear if the batch normalization operation, added after each operation by default, is optimal, and our approach is flexible to cover this option by adding one more set in factorization. Also, convolutional operations have orthogonal properties, *e.g.*, different convolution types (*e.g.*, normal, separable, dilated, *etc.*) combined with different kernel sizes, and factorizing them into smaller sets can improve automation of architecture search, which meets the intention of AutoML [55]. Topics are left for future work.

## References

- [1] Jonathan T. Barron. Continuously differentiable exponential linear units. *arXiv preprint arXiv:1704.07483*, 2017. 3
- [2] Kaifeng Bi, Changping Hu, Lingxi Xie, Xin Chen, Longhui Wei, and Qi Tian. Stabilizing DARTS with amended gradient estimation on architectural parameters. *arXiv preprint arXiv:1910.11831*, 2019. 2, 4, 9
- [3] Han Cai, Tianyao Chen, Weinan Zhang, Yong Yu, and Jun Wang. Efficient architecture search by network transformation. In *AAAI*, 2018. 2
- [4] Han Cai, Ligeng Zhu, and Song Han. Proxylessnas: Direct neural architecture search on target task and hardware. *arXiv preprint arXiv:1812.00332*, 2018. 5, 7
- [5] Xin Chen, Lingxi Xie, Jun Wu, and Qi Tian. Progressive differentiable architecture search: Bridging the depth gap between search and evaluation. In *ICCV*, 2019. 2, 5, 6, 7
- [6] Djork-Arné Clevert, Thomas Unterthiner, and Sepp Hochreiter. Fast and accurate deep network learning by exponential linear units(elus). In *ICLR*, 2016. 3
- [7] Ekin D. Cubuk, Barret Zoph, Dandelion Mane, Vijay Vasudevan, and Quoc V. Le. Autoaugment: Learning augmentation strategies from data. In *CVPR*, 2019. 2, 8
- [8] Jia Deng, Wei Dong, Richard Socher, Li-Jia Li, Kai Li, and Fei-Fei Li. Imagenet: A large-scale hierarchical image database. In *CVPR*, 2009. 5, 7
- [9] Terrance Devries and Graham W. Taylor. Improved regularization of convolutional neural networks with cutout. *arXiv preprint arXiv:1708.04552*, 2019. 5
- [10] Xuanyi Dong and Yi Yang. Searching for a robust neural architecture in four GPU hours. In *CVPR*, 2019. 2
- [11] Thomas Elsken, Jan Hendrik Metzen, and Frank Hutter. Simple and efficient architecture search for convolutional neural networks. In *ICLR*, 2018. 2
- [12] Thomas Elsken, Jan Hendrik Metzen, and Frank Hutter. Efficient multi-objective neural architecture search via lamarckian evolution. In *ICLR*, 2019. 1, 2
- [13] Golnaz Ghiasi, Tsung-Yi Lin, and Quoc V. Le. NAS-FPN: learning scalable feature pyramid architecture for object detection. In *CVPR*, 2019. 1
- [14] Zichao Guo, Xiangyu Zhang, Haoyuan Mu, Wen Heng, Zechun Liu, Yichen Wei, and Jian Sun. Single path one-shot neural architecture search with uniform sampling. *arXiv preprint arXiv:1904.00420*, 2019. 1
- [15] Kaiming He, Xiangyu Zhang, Shaoqing Ren, and Jian Sun. Delving deep into rectifiers: Surpassing human-level performance on imagenet classification. In *ICCV*, 2015. 3
- [16] Kaiming He, Xiangyu Zhang, Shaoqing Ren, and Jian Sun. Deep residual learning for image recognition. In *CVPR*, 2016. 2
- [17] Andrew Howard, Mark Sandler, Grace Chu, Liang-Chieh Chen, Bo Chen, Mingxing Tan, Weijun Wang, Yukun Zhu, Ruoming Pang, Vijay Vasudevan, Quoc V. Le, and Hartwig Adam. Searching for mobilenetv3. *arXiv preprint arXiv:1905.02244*, 2019. 2
- [18] Andrew G Howard, Menglong Zhu, Bo Chen, Dmitry Kalenichenko, Weijun Wang, Tobias Weyand, Marco Andreetto, and Hartwig Adam. Mobilenets: Efficient convolutional neural networks for mobile vision applications. *arXiv preprint arXiv:1704.04861*, 2017. 7
- [19] Jie Hu, Li Shen, and Gang Sun. Squeeze-and-excitation networks. In *CVPR*, 2018. 8
- [20] Gao Huang, Zhuang Liu, Laurens Van Der Maaten, and Kilian Q Weinberger. Densely connected convolutional networks. In *CVPR*, 2017. 2, 5
- [21] Gao Huang, Yu Sun, Zhuang Liu, Daniel Sedra, and Kilian Q. Weinberger. Deep networks with stochastic depth. In *ECCV*, 2016. 5
- [22] Diederik P. Kingma and Jimmy Ba. Adam: A method for stochastic optimization. In *ICLR*, 2015. 5, 8
- [23] Günter Klambauer, Thomas Unterthiner, Andreas Mayr, and Sepp Hochreiter. Self-normalizing neural networks. In *NeurIPS*, 2017. 3
- [24] Alex Krizhevsky. Convolutional deep belief networks on cifar-10. Technical report, 2015. 3
- [25] A. Krizhevsky and G. Hinton. Learning multiple layers of features from tiny images. *Computer Science Department, University of Toronto, Tech. Rep.*, 1, 01 2009. 5
- [26] Alex Krizhevsky, Ilya Sutskever, and Geoffrey E. Hinton. Imagenet classification with deep convolutional neural networks. In *NeurIPS*, 2012. 2

- [27] Gustav Larsson, Michael Maire, and Gregory Shakhnarovich. Fractalnet: Ultra-deep neural networks without residuals. In *ICLR*, 2017. 5
- [28] Chenxi Liu, Liang-Chieh Chen, Florian Schroff, Hartwig Adam, Wei Hua, Alan L. Yuille, and Fei-Fei Li. Auto-deeplab: Hierarchical neural architecture search for semantic image segmentation. In *CVPR*, 2019. 1
- [29] Chenxi Liu, Barret Zoph, Maxim Neumann, Jonathon Shlens, Wei Hua, Li-Jia Li, Li Fei-Fei, Alan Yuille, Jonathan Huang, and Kevin Murphy. Progressive neural architecture search. In *EECV*, 2018. 1, 2, 4, 5, 7
- [30] Hanxiao Liu, Karen Simonyan, Oriol Vinyals, Chrisantha Fernando, and Koray Kavukcuoglu. Hierarchical representations for efficient architecture search. *arXiv preprint arXiv:1711.00436*, 2017. 5
- [31] Hanxiao Liu, Karen Simonyan, and Yiming Yang. DARTS: differentiable architecture search. In *ICLR*, 2019. 1, 2, 4, 5, 7
- [32] Renqian Luo, Fei Tian, Tao Qin, Enhong Chen, and Tie-Yan Liu. Neural architecture optimization. In *Advances in neural information processing systems*, 2018. 5
- [33] Ningning Ma, Xiangyu Zhang, Hai-Tao Zheng, and Jian Sun. Shufflenet v2: Practical guidelines for efficient cnn architecture design. In *ECCV*, 2018. 7
- [34] Awni Y. Maas, Andrew L. and Hannun and Andrew Y. Ng. Rectifier nonlinearities improve neural network acoustic models. In *ICML*, 2013. 3
- [35] Vinod Nair and Geoffrey E. Hinton. Rectified linear units improve restricted boltzmann machines. In *ICML*, 2010. 3
- [36] Hieu Pham, Melody Y Guan, Barret Zoph, Quoc V Le, and Jeff Dean. Efficient neural architecture search via parameter sharing. *arXiv preprint arXiv:1802.03268*, 2018. 1, 2, 5
- [37] Prajit Ramachandran, Barret Zoph, and Quoc V. Le. Searching for activation functions. In *ICLR*, 2018. 2, 3, 4, 6
- [38] Esteban Real, Alok Aggarwal, Yanping Huang, and Quoc V Le. Regularized evolution for image classifier architecture search. In *AAAI*, 2019. 1, 2, 5, 7
- [39] Esteban Real, Sherry Moore, Andrew Selle, Saurabh Saxena, Yutaka Leon Suematsu, Jie Tan, Quoc V. Le, and Alexey Kurakin. Large-scale evolution of image classifiers. In *ICML*, 2017. 1, 2
- [40] Olga Russakovsky, Jia Deng, Hao Su, Jonathan Krause, Sanjeev Satheesh, Sean Ma, Zhiheng Huang, Andrej Karpathy, Aditya Khosla, Michael S. Bernstein, Alexander C. Berg, and Fei-Fei Li. Imagenet large scale visual recognition challenge. *International Journal of Computer Vision*, 115(3):211–252, 2015. 7
- [41] Mark Sandler, Andrew G. Howard, Menglong Zhu, Andrey Zhmoginov, and Liang-Chieh Chen. Mobilenetv2: Inverted residuals and linear bottlenecks. In *CVPR*, 2018. 2
- [42] Albert Shaw, Daniel Hunter, Forrest N. Iandola, and Sammy Sidhu. Squeezenas: Fast neural architecture search for faster semantic segmentation. *arXiv preprint arXiv: 1908.01748*, 2019. 2
- [43] Christian Szegedy, Wei Liu, Yangqing Jia, Pierre Sermanet, Scott Reed, Dragomir Anguelov, Dumitru Erhan, Vincent Vanhoucke, and Andrew Rabinovich. Going deeper with convolutions. In *CVPR*, 2015. 7
- [44] Christian Szegedy, Vincent Vanhoucke, Sergey Ioffe, Jonathon Shlens, and Zbigniew Wojna. Rethinking the inception architecture for computer vision. In *CVPR*, 2016. 8
- [45] Mingxing Tan, Bo Chen, Ruoming Pang, Vijay Vasudevan, Mark Sandler, Andrew Howard, and Quoc V Le. Mnasnet: Platform-aware neural architecture search for mobile. In *CVPR*, 2019. 2, 7
- [46] Mingxing Tan and Quoc V. Le. Efficientnet: Rethinking model scaling for convolutional neural networks. In *ICML*, 2019. 1
- [47] Bichen Wu, Xiaoliang Dai, Peizhao Zhang, Yanghan Wang, Fei Sun, Yiming Wu, Yuandong Tian, Peter Vajda, Yangqing Jia, and Kurt Keutzer. Fbnet: Hardware-aware efficient convnet design via differentiable neural architecture search. In *CVPR*, 2019. 2
- [48] Lingxi Xie and Alan L. Yuille. Genetic cnn. In *ICCV*, 2017. 1, 2
- [49] Sirui Xie, Hehui Zheng, Chunxiao Liu, and Liang Lin. Snas: stochastic neural architecture search. *arXiv preprint arXiv:1812.09926*, 2018. 5, 7
- [50] Bing Xu, Naiyan Wang, Tianqi Chen, and Mu Li. Empirical evaluation of rectified activations in convolutional network. *arXiv preprint arXiv:1505.00853*, 2015. 3
- [51] Peng Xu, Yongye Huang, Tongtong Yuan, Kaiyue Pang, Yi-Zhe Song, Tao Xiang, Timothy M. Hospedales, Zhanyu Ma, and Jun Guo. Sketchmate: Deep hashing for million-scale human sketch retrieval. In *CVPR*, 2018. 2
- [52] Yuhui Xu, Lingxi Xie, Xiaopeng Zhang, Xin Chen, Guo-Jun Qi, Qi Tian, and Hongkai Xiong. Pc-darts: Partial channel connections for memory-efficient differentiable architecture search. *arXiv preprint arXiv:1907.05737*, 2019. 2, 5, 6, 7, 8
- [53] Arber Zela, Thomas Elsken, Tonmoy Saikia, Yassine Marrakchi, Thomas Brox, and Frank Hutter. Understanding and robustifying differentiable architecture search. *arXiv preprint arXiv:1909.09656*, 2019. 2, 4, 9
- [54] Hongpeng Zhou, Minghao Yang, Jun Wang, and Wei Pan. Bayesnas: A bayesian approach for neural architecture search. In *ICML*, 2019. 5, 7
- [55] Marc-André Zöllner and Marco F. Huber. Survey on automated machine learning. *arXiv preprint arXiv:1904.12054*, 2019. 9
- [56] Barret Zoph and Quoc V. Le. Neural architecture search with reinforcement learning. In *ICLR*, 2017. 1, 2
- [57] Barret Zoph, Vijay Vasudevan, Jonathon Shlens, and Quoc V Le. Learning transferable architectures for scalable image recognition. In *CVPR*, 2018. 1, 2, 5, 7